LATTICE GAS METHODS FOR PREDICTING INTRINSIC PERMEABILITY OF POROUS MEDIA.

L.O. E. Santos[+], emerich@lmpt.ufsc.br
P.C. Philippi[+•], philippi@lmpt.ufsc.br
M.C. Damiani[*], damiani@lmpt.ufsc.br

(+) Porous Media and Thermophysical Properties Laboratory (LMPT).
Mechanical Engineering Department. Federal University of Santa Catarina
88040-900 Florianópolis, SC, Brazil.
(*) Engineering Simulation and Scientific Software (ESSS)
Parque Tecnológico de Florianópolis - Rodovia SC 401 km 001
88030-000 Florianópolis , SC, Brasil

Abstract. This paper presents a method for predicting intrinsic permeability of porous media based on Lattice Gas Cellular Automata methods. Two methods are presented. The first is based on a Boolean model (LGA). The second is Boltzmann method (LB) based on Boltzmann relaxation equation. LGA is a relatively recent method developed to perform hydrodynamic calculations. The method, in its simplest form, consists of a regular lattice populated with particles that hop from site to site in discrete time steps in a process, called *propagation*. After propagation, the particles in each site interact with each other in a process called *collision*, in which the number of particles and momentum are conserved. An exclusion principle is imposed in order to achieve better computational efficiency. In despite of its simplicity, this model evolves in agreement with Navier-Stokes equation for low Mach numbers. LB methods were recently developed for the numerical integration of the Navier-Stokes equation based on discrete Boltzmann transport equation. Derived from LGA, LB is a powerful alternative to the standard methods in computational fluid dynamics. In recent years, it has received much attention and has been used in several applications like simulations of flows through porous media, turbulent flows and multiphase flows. It is important to emphasize some aspects that make Lattice Gas Cellular Automata methods very attractive for simulating flows through porous media. In fact, boundary conditions in flows through complex geometry structures are very easy to describe in simulations using these methods. In LGA methods simulations are performed with integers needing less resident memory capability and boolean arithmetic reduces running time. The two methods are used to simulate flows through several Brazilian reservoir petroleum rocks leading to intrinsic permeability prediction. Simulation is compared with experimental results.

Keywords: *fluid flow, porous media, permeability, lattice-gas*

• Corresponding Author

1. INTRODUCTION

Lattice gas models (LGA) designate a large class of models whose main feature is the presence of a set of particles moving in a discrete space (a lattice). The use of such models to study and simulate fluid dynamics was firstly introduced by J. Hardy, O. de Pazzis e Y. Pomeau, in 1973, Hardy *et al.* (1973), but it was only after 1986 that these models grew in increased importance due to the work of Frisch *et al.* (1986, 1987). These authors formally demonstrated that, under certain conditions, the dynamics of such models was described by the Navier-Stokes equations for incompressible flows, and could be used to simulate such flows. Since then, several improvements have been made to simulate multiphase flows (Rothmann and Keller, 1988, Chen *et al.,* 1991), phase transitions (Apppert and Zaleski, 1990) and the development of a new method to simulate fluid dynamics: the Lattice-Boltzmann Method (McNamara. and Zanetti, 1988, Higera and Jimenez, 1989, Qian, d'Humières, Lallemand, 1992).

Although computer non-expensive, considering processing operations and resident memory requirements, lattice gas cellular automata (LGA) have intrinsic fluctuations related to the use of Boolean variables and is not suitable for describing hydrodynamics, excepting in the limit of incompressible, low Reynolds number flows (Rothman and Zaleski, 1997**)**. In fact, the equilibrium distribution for the expected values of the Boolean variables, used in these models, is a Fermi-Dirac distribution, producing non-physical effects for intermediates and large Reynolds number.

Lattice Boltzmann method (LB) was originated from the ensemble average of LGA microscopic dynamic equation. In this aspect: i) it is based on regular discrete lattices, maintaining propagation and collision steps, ii) it works with real variables instead of Boolean variables, which are interpreted as the probability $N_i(X,T)$ of finding a particle in the direction *i* of a given lattice site **X**, at time T.

The main feature of Boltzmann method, distinguishing this method from a method based on statistical ensemble averages of Boolean models, is that the collision term is written to give the expected macroscopic behavior.

In this way LB method is not limited to low Reynolds number flows, being suitable to the study of flow problems where inertial effects are important. In fact, it has been used in the last decade in the study of unstable flows with periodic fluctuations (von Karman vortex street).

This work is devoted to present the single phase lattice gas models giving rise to LGA and LB methods, which are applied to estimate the intrinsic permeability of sandstones. The microscopic and macroscopic dynamics are discussed. Simulation results are presented and compared with experimental values in the prediction of intrinsic permeability of Brazilian sandstones.

2. BOOLEAN MODEL

2.1 Microscopic Dynamics

Lattice gas models are, basically, composed by particles distributed over a discrete space, the nodes of a regular lattice (Bravais lattice). The particles hop from a site to the neighbor sites in one time step with a discrete and limited velocities' set.

In LGA models, the state of a site X at time T is represented by a set of Boolean variables, designating the presence (n_i=1) or absence (n_i=0) of a particle in a given direction i, n_0 indicates the presence or absence of a rest particle. For each time step, the dynamical evolution of the model is given in two steps. In the first step, designated as *collision step*, the state of site X is changed following collision rules conceived so as to preserve total mass and momentum of the site. In the second step, called *propagation step*, particles are propagated to the neighbor sites, in accordance with their direction at site X after collision step. This is described by the evolution equation:

$$n_i(\mathbf{X}+\mathbf{c}_i, T+1)=n_i(\mathbf{X},T) + \omega_i(n_1,...n_b), \quad (1)$$

where ω_i: $(n_1,...n_b)\rightarrow\{-1,0,1\}$ represents the collision operator which can take the values –1, 1 or 0, depending on the state $(n_1,...n_b)$ of site X before the collision. Considering S to be the set of 2^b possible states, $s=(s_1,...s_b)$ of site X and α: SXS $\rightarrow$ [0,1], to be the transition matrix (with 2^b X2^b elements), the collision operator can be written as

$$\omega_i(n_1,...,n_b)=\sum_s\left[\sum_{s'}\alpha(s,s')(s'_i-s_i)\prod_{j=1}^{b}\delta(n_{j+i},s_{j+i})\right], \quad (2)$$

where s' designates post collision states. In present work, it was considered changes to each possible state s' with the same probability with the inclusion of s between the post collision states.

2.2 The FCHC model

Simulation results presented in this paper are based on the three-dimensional FCHC model (d'Humières *et al*., 1986). Three-dimensional regular lattices do not have the required symmetries and fail in describing fluid flow with isotropic properties. To overcome this problem d'Humières*, et al.* proposed the use of the face centered hipercubic lattice (FCHC). This lattice is constructed using the vectors:

$$\mathbf{c}_i = \text{perm}(\pm1,\pm1,0,0), \quad (3)$$

where the symbol "*perm*(a,b,c,d)" indicates all the permutations among a,b,c,d. There are six possible permutations and four combination of signs and, consequently, 24 vectors $\mathbf{c}_i$. Considering the three dimensional projection of FCHC lattice (i. e. the first three dimensions), two kinds of vectors are possible. Twelve vectors have the form

$$\mathbf{c}_i = perm(\pm1,\pm1,0), \quad (4)$$

whose moduli are $\sqrt{2}$. These vectors will connect second neighbors in the three dimensional projection.

The remaining twelve vectors have the form

$$\mathbf{c}_i = perm(\pm1,0,0), \quad (5)$$

and correspond to vectors linking the first neighbors in the projection. It is important to notice that each projected vector of this form is the result of the projection of one of the two possible vectors in the four dimensional lattice:

$$\mathbf{c}_i = (perm(\pm1,0,0),1), \quad (6)$$

and

$$\mathbf{c}_i = (perm(\pm1,0,0),-1), \quad (7)$$

therefore it is necessary to use two vectors linking the first neighbors in 3D projection, i. e., two particles are allowed to populate each of these directions.

2.3 Forcing the Flow

External body forces **g(X)** may be simulated in LGA by adding a fixed amount of momentum at site X at each unitary time step. In present paper, this is performed after each collision step, by changing n_i by

$$\Delta n_i^g = P(X)\{g_i[n_i(1-n_{i+b/2})-n_{i+b/2}(1-n_i)]+g_{i+b/2}[n_{i+b/2}(1-n_i)-n_i(1-n_{i+b/2})]\}, \quad (8)$$

whenever possible, i.e., whenever exclusion principle is not violated and mass is preserved, P(**X**) being 1 when a random variable attributed to **X** is smaller than S(**X**) and 0 otherwise, in accordance with a given probability S(X), related to the external force strength. Eq. (1) is thus, modified, to give:

$$n_i(\mathbf{X}+\mathbf{c}_i, T+1)=n_i(\mathbf{X},T)+\omega_i(n_1,...n_b)+\Delta n_i^g. \quad (9)$$

2.4 Boltzmann Approximation

Lattice gas simulation may be considered as a single realization of a stochastic process, starting from a given initial condition. Considering an *ensemble* of different realizations and calling

$$N_i=<n_i(\mathbf{X},T)>, \tag{10}$$

corresponding to the expected value of the Boolean variable n_i at a given point X and time T, the evolution equation satisfied by N_i can be found, at a closed form, by supposing Boolean variables n_i at X, T to be non-correlated before collision. This is called *molecular chaos* hypothesis and gives

$$N_i(\mathbf{X}+\mathbf{c}_i, T+1) - N_i(\mathbf{X},T)= \Omega_i = \sum_s \left[\sum_{s'} A(s,s')(s'_i - s_i) \prod_{j=1}^{b} \delta(N_{j+i}, s_{j+i}) \right], \tag{11}$$

which is the dynamical evolution equation for the distribution N_i, in the Boltzmann approximation.

In the above equation,

$$\Omega_i = < \omega_i(n_1,...,n_b) >, \tag{12}$$

$$A(s, s')= <\alpha(s, s')>, \tag{13}$$

Using the semi-detailed balance condition, it may be proved that,

$$\sum_s A(s,s') = 1 \qquad \forall s'. \tag{14}$$

Equation (11) has an H-Theorem and an equilibrium solution, which is a Fermi-Dirac distribution function

$$N_i^o = \frac{1}{1+\exp(h+\mathbf{q}.\mathbf{c}_i)}. \tag{15}$$

Due to the discrete nature of the model, a linear low velocity approximation of Eq.(15) is used, written in terms of the density

$$\rho = \sum_{i=1}^{b_m} N_i + N_o b_r, \tag{16}$$

where b_r is the maximum number of rest particles allowed at each site X, and in terms of the mean velocity

$$\mathbf{u} = \frac{1}{\rho} \sum_{i=1}^{b_m} N_i \mathbf{c}_i. \tag{17}$$

This equilibrium solution can be written as

$$N_i^o = f\left[1 + \frac{Db}{c^2 b_m} c_{i\alpha} u_\alpha + \frac{D^2}{2c^4} \frac{b^2}{b_m^2} \left(\frac{1-2f}{1-f} \right) \left(c_{i\alpha} c_{i\beta} - \frac{c^2}{D}(1-b_r)\delta_{\alpha\beta} \right) u_\alpha u_\beta \right] + O(u^3) \tag{18}$$

for moving particles whereas for rest particles,

$$N_o^o = f\left[1 - \frac{D}{2c^2} \frac{b}{b_m} \left(\frac{1-2f}{1-f} \right) u^2 \right] + O(u^4) \tag{19}$$

In the above equations D is the Euclidean dimension of the lattice, D=2 in FHP and D=4 in FCHC models, $b= b_m + b_r$ and $f=\rho/b$.

2.5 Scaling to physical variables

Using h and ε as, respectively, a spatial and a time scale

$$\begin{aligned} \mathbf{x} &= h\mathbf{X} \\ t &= \delta T \end{aligned}, \tag{20}$$

x and t may be considered as physical variables, varying continuously in the spatial and time domain of the physical system to be described, when h and δ are small.

2.6 Lattice Gas Hydrodynamic Equations

Use of Chapman-Enskog method on the N_i evolution equation, Eq.(6), leads to lattice gas hydrodynamic equations, in the limit of low Knudsen number Kn=h/L=δ/Γ<<1, where L is a characteristic length and Γ is a characteristic time:

$$\partial_t(\rho) + \partial_\beta(\rho u_\beta) = 0 \tag{21}$$

$$\partial_t(\rho u_\alpha) + \partial_\beta\left[g(\rho)\rho u_\alpha u_\beta\right] = \partial_\alpha(p(\rho, u^2)) + \nu\partial_\beta\left[\partial_\beta(\rho u_\alpha) + \partial_\alpha(\rho u_\beta)\right] + \eta\partial_\alpha\left[\partial_\beta(\rho u_\beta)\right] \tag{22}$$

where

$$g(\rho) = \frac{2}{3}\left(\frac{1-\rho/12}{1-\rho/24}\right) \tag{23}$$

$$p(\rho, u^2) = c_s{}^2\rho - \frac{5}{4}M^2\rho g(\rho) \tag{24}$$

and $c_s{}^2 = \frac{1}{2}$ is the square of LGA sound speed. The first and the second viscosity coefficients, respectively ν and η, are related to the eigenvalues of collision operator **Ω.** Equations (21)-(22) differ from Navier-Stokes hydrodynamic equations: i) by the inclusion of a g(ρ) dependence in the inertial term, breaking Galilean invariance, ii) taking M as the Mach number, $M = U/c_s$, by a $O(M^2)$ additional term in the pressure equation (Eq.(24)) and iii) by the inclusion of density ρ *inside* the spatial derivatives in the viscous terms. These *non- physical lattice effects* disappear in the low Reynolds, Re = U L/ν and Mach numbers, $M = U/c_s$, limits. This was demonstrated by Rothman and Zaleski (1997) by using *perturbation analysis* and the correct hydrodynamic equations are found when M<<Re<<1:

$$\rho\partial_t(u_\alpha) = \partial_\alpha(p) + \rho\nu\partial_\beta\partial_\beta u_\alpha \tag{25}$$

which is the momentum equation for low Reynolds number incompressible flows.

2.7 Boundary conditions

Collision step uses local information only and therefore, boundary conditions are introduced, solely, in the propagation step. In the sites near the wall, all particles that would hit the walls have their velocity reversed, during this step: $\mathbf{c}_i \rightarrow -\mathbf{c}_i$. This is called a *bouncing-back* boundary condition. Bouncing-back restriction leads to non-slip boundary condition at the wall.

In the inlet and outlet regions periodic boundary conditions are used: every particle exiting the simulation region from one edge is injected into the other edge with the same velocity. In the simulations of flows through porous media non-solid regions were added in the inlet and the outlet boundaries in order to guarantee that a particle exiting the lattice will never encounters a wall in the other edge. These non-solid region were also used to force the flow in the interested region, acting as hydraulic pumps to compensate head loss produced by porous structure

3. BOLTZMANN METHOD

3.1 Microscopic Dynamics

Three-dimensional physical space is considered to be a cubic lattice where each site **X** has b_m neighbors. Each site is characterized by a particle distribution function $N_i(\mathbf{X},T)$ which evolves according to the Lattice Boltzmann Equation:

$$N_i(\mathbf{X} + \mathbf{c}_i, T+1) - N_i(\mathbf{X} + \mathbf{c}_i, T+1) = \Omega_i, \tag{26}$$

where T is the time variable, the index *i* indicates the neighbor, $\mathbf{c}_i$ is a velocity vector pointing to neighbor *i* (*i=0* refers to the rest particle distribution). The term in the right side is called collision term and is writen in such way that

$$\sum_{i=0}^{b_m} \Omega_i = 0, \tag{27}$$

$$\sum_{i=0}^{b_m} \Omega_i \mathbf{c}_i = 0, \tag{28}$$

in order to preserve the mass and momentum of each site.

The evolution of the model, given by equation (26), can be split in two processes. In the first, designated as *collision*, the distribution function $N_i(\mathbf{X}, T)$ is changed by the action of the collision operator. In the second process, called *propagation*, the values N_i are propagated to the neighbor sites, in accordance with the direction of the vector $\mathbf{c}_i$.

The mass and momentum variables are defined with the help of the distribution function:

$$\sum_{i=1}^{b_m} N_i + N_0 = \rho, \tag{29}$$

$$\sum_{i=0}^{b_m} N_i \mathbf{c}_i = \rho \boldsymbol{u}. \tag{30}$$

3.2 The BGK Collision Term

In present paper a single-time-relaxation approximation for the collision is used (BGK model (Qian *et al.,* 1992)

$$\Omega_i = \frac{(N_i^{eq} - N_i)}{\tau}, \tag{31}$$

where τ is the relaxation time and N_i^{eq}, the equilibrium distribution, is determined in order to obtain the desired macroscopic equations. The rate of change toward the equilibrium distribution is imposed to produce the viscosity of the fluid, which is the only macroscopic property related to collisions in single-fluid flows.

3..3 Equilibrium distributions

When equilibrium is reached collision process should not affect the particle distribution. Therefore, the equilibrium distributions N_i^{eq} must be specified by the collisional invariants ρ and $\underline{\mathbf{u}}$. In the case of small **u**, it can be written:

$$N_i^{eq}(\rho, \mathbf{u}) = A_i + B_{i\alpha}\mathbf{u}_\alpha + D_{i\alpha\beta}\mathbf{u}_\alpha\mathbf{u}_\beta \qquad i=1,2,\ldots,b_m \tag{32}$$

where b_m indicates the number of directions of the lattice.

There are some conditions that must be imposed to N_i^{eq} in order to determine A_i, $B_{i\alpha}$ and $D_{i\alpha\beta}$. First, it is imposed that any transformation that preserves the lattice and direction *i* must not affect the equilibrium distribution, rest particles equilibrium distributions must be independent of the direction **i**, the distributions N_i^{eq} and N_0^{eq} must be in accordance with equations (29) and (30) and equilibrium distribution must retrieve macroscopic hydrodynamic equations, avoiding non-physical lattice gas effects.

It can be shown that, equilibrium distribution for the rest particles is given by

$$N_0^{eq} = \rho\left(\frac{b_r}{b_r + b_m}\right) - \frac{\rho}{2}(\boldsymbol{u})^2, \tag{33}$$

and for moving particles along the main axes

$$N_i^{eq} = \rho\left(\frac{1}{br + bm}\right) + \rho\left(\frac{2}{b_m}\right)\mathbf{c}_i \cdot \boldsymbol{u} + \rho\left(\frac{3}{b_m}\right)(\mathbf{c}_i \cdot \boldsymbol{u})^2 - \rho\left(\frac{1}{b_m}\right)(\boldsymbol{u})^2, \tag{34}$$

and for particles moving along the diagonals $\left(|\mathbf{c}_i| = \sqrt{2}\right)$, N_i^{eq} is given by

$$N_i^{eq} = \frac{\rho}{2}\left(\frac{1}{br + bm}\right) + \frac{\rho}{2}\left(\frac{2}{b_m}\right)\mathbf{c}_i \cdot \boldsymbol{u} + \frac{\rho}{2}\left(\frac{3}{b_m}\right)(\mathbf{c}_i \cdot \boldsymbol{u})^2 - \frac{\rho}{2}\left(\frac{1}{b_m}\right)(\boldsymbol{u})^2. \tag{35}$$

3.4 Hydrodynamic LB equations

Using Chapman-Enskog method, in the limit of low Knudsen number Kn=h/L=δ/Γ<<1, where L is a characteristic length and Γ is a characteristic time and neglecting terms beyond second order, leads to

$$\partial_t(\rho) + \partial_\beta(\rho u_\beta) = 0 \tag{36}$$

$$\partial_t(\rho u_\alpha) + \partial_\beta(\rho u_\alpha u_\beta) = -\partial_\alpha(p) + \nu\partial_\beta\left[\partial_\beta(\rho u_\alpha) + \partial_\alpha(\rho u_\beta)\right] \tag{37}$$

where the pressure p and the kinematic viscosity ν are given by

$$p = \frac{1}{3}\rho \tag{38}$$

$$\nu = \frac{1}{6}(2\tau - 1). \tag{39}$$

The mass balance equation is, exactly, the same equation obtained in classical hydrodynamics. Considering low Mach number (ρ constant), the obtained momentum balance equation will be, clearly, in agreement with the Navier-Stokes equation.

3.5 Boundary conditions

The non-slip condition near the walls can be easily obtained imposing the bouncing-back boundary condition, i. e., all particle that would hit the walls in the propagation step reverses its direction in this step. There are other (and more precise) ways to ensure non-slip condition (Zou He, 1997), but the bouncing-back boundary condition was chosen due to its simplicity.

In the simulations periodic boundary conditions were always used. For simulating flows through porous media it was added a non-solid region in the inlet and outlet, and flow was forced adding some amount of momentum at each site of this region, according to the equation

$$N_i(X + \mathbf{c}_i, T + 1) - N_i(X + \mathbf{c}_i, T + 1) = \Omega_i + \mathbf{f} \cdot \mathbf{c}_i \tag{40}$$

where **f** indicates the direction of the force applied and is proportional to its magnitude.

4. RESULTS

Several simulations were performed to calculate intrinsic permeability of Brazilian sandstones. Simulations start from three-dimensional representations of the porous structure, reconstructed from petrographic thin plates by using Liang *et al*. method (Liang *et al*., 1998). Segmentation methods provide binary two-dimensional images, from digital color and/or gray-level images. Three-dimensional reconstruction is based on the generation of three-dimensional stochastic realizations, preserving the statistical moments of phase function, which are measured on the target binary image. Present reconstruction method preserves the two first moments of the phase function: porosity and auto-correlation. A main reconstruction parameter is the sampling factor 'n'. Sampling factor n=1 means that three-dimensional representation and the binary image have the same spatial resolution. As sampling factor n increases, resolution decays with the same ratio. In general, it is very difficult to preserve original resolution, in reconstructed representations, due to

limitations inherent to the reconstruction method itself, which fails in preserving the fine details of the porous structure. In this sense, the best reconstructed microstructure is considered to be the one generated with the sampling factor that gave the best agreement between pore size distributions, measured on the original binary image and on cross-sections of the three-dimensional representation. Further details can be found in Liang *et al*. (1998) and Damiani *et al.* (2000). Table I gives some simulation results and comparison with experimental data for Brazilian sandstones. Best sampling factor is indicated by an (*). Another important reconstruction parameter is the 3D representation linear size N. Size N must be great enough to assure statistical homogeneity, with respect to fluid flow problem. Nevertheless, computer resident memory requirements are multiplied by 8, when N doubles. In this way, considering computer limitations, simulation starts from small and proceeds to larger linear sizes until convergence.

Table I - Simulation results and comparison with experimental data (Experimental data and source digital images where furnished by CENPES/ Petrobras)

Sandstone Sample	Experimental Permeability	Reconstructed Image Linear Size (N)	Sampling Factor (n)	Simulated Permeability LB	Simulated Permeability LGA
P26.2K441	441	100	6	-	469
P26.2K441	441	100	5 (*)	743	368
P26.2K441	441	150	5 (*)	709	-
P26.2K441	441	200	5 (*)	-	462
P23.8K145	145	150	3	-	218
P23.8K145	145	100	4 (*)	-	238
P23.8K145	145	150	4 (*)	-	256
P26.2K69.7	69.7	150	2 (*)	-	90
P26.2K69.7	69.7	200	2 (*)	-	77
P22.3K154	154	100	4	-	55
P22.3K154	154	100	5	-	64
P22.3K154	154	100	6 (*)	-	81
P27.5K316	316	100	4	-	261
P27.5K316	316	100	5	458	238
P27.5K316	316	150	5	350	-
P27.5K316	316	100	6 (*)	-	316

(*) Best sampling factor

5. DISCUSSION AND CONCLUSIONS

Although based on a simpler model, Boolean method gave the best results when compared to Boltzmann method, in predicting intrinsic permeability of porous rocks. This result may appear as surprising for all those familiar with Lattice Gas Cellular Automata methods, but not acquainted with the intrinsic difficulties in working with 3D representations of porous structures.

In fact, difficulty in predicting flow through porous structures is increased due to the presence of small constrictions spatially distributed inside the whole structure. In usual representations these constrictions appear with, only, some few voxels width.

Boltzmann method cannot predict reliable values for the velocity field inside these constrictions as it is based on the *relaxation* of a distribution function to a *collision based* equilibrium distribution, written so as to satisfy *continuum* macroscopic equations. In fact, recent works have show that the number of sites between constriction walls must be larger than 20, when applying Boltzmann method. In this way if we want to enlarge, e.g., a 2 voxels diameter small

channel to 20 voxels, the linear size N must be multiplied by a factor of 10. This increases computer storage needs by a factor of 10^3!

Nevertheless, fluid flow is very ineffective through small constrictions and main flow follows the trajectory that offers the smallest hydraulic resistance (Fig. 1).

The main question to be answered is related to the suitability of increasing linear size to improve the accuracy in simulating flow through these small constrictions, considering their small role in producing hydraulic permeability.

On the other way, LGA method is based on particle collisions and does not requires any equilibrium distribution to be run. In addition, although bouncing back condition increases hydraulic resistance through constrictions, with respect to Knudsen flow, *main flow* is, apparently, correctly modeled, producing reliable values of intrinsic permeability

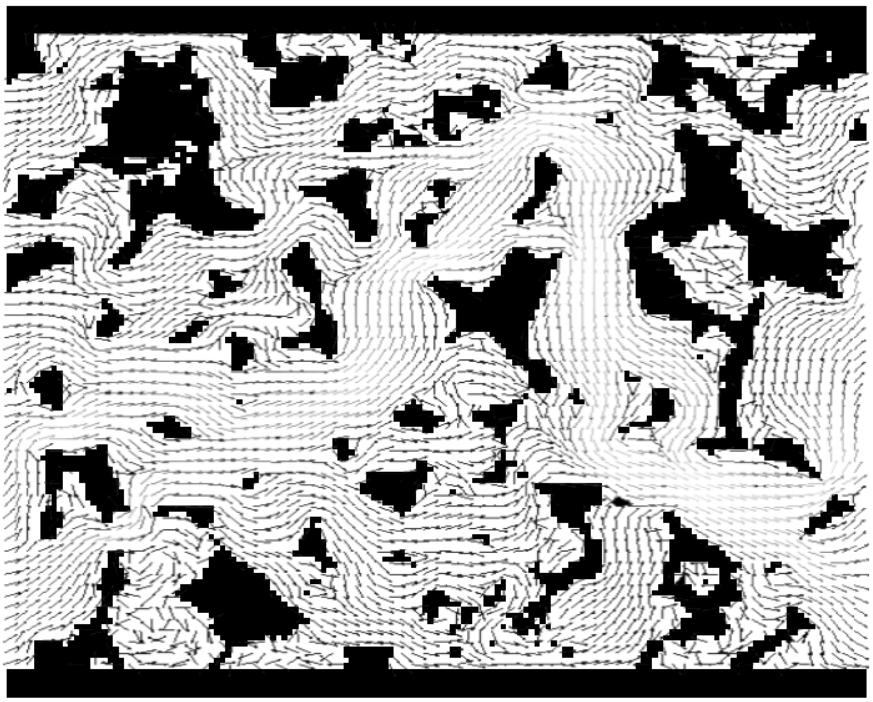

Figure 1 Local velocity field inside a two dimensional porous space, illustrating main flow line (brighter lines correspond to higher speeds).

Acknowledgements. The authors would like to acknowledge CENPES/PETROBRAS (Centro de Pesquisas e Desenvolvimento Leopoldo A. Miguez de Mello) for providing the images and experimental data for Berea and Brazilian sandstones and the financial support of CNPq (Conselho Nacional de Desenvolvimento Científico e Tecnológico), PADCT (Programa de Apoio ao Desenvolvimnto Científico e Tecnológico), RHAE (Programa de Formação de Recursos Humanos em Areas Estratégicas) and FINEP (Financiadora de Estudos e projetos).

REFERENCES

Appert, C. and Zaleski, 1990, A lattice gas liquid-gas transition, Physical Review Letters **64**, 1-4.

Chen, S., Doolen G. D., Eggert, K., Grunau, D. and Loh, E. Y., 1991, Local lattice-gas model for immiscible fluids, Physical Review A **43,** 7053-7056.

Damiani, M. C., Fernandes, C. P., Bueno, A. D., Santos, L. O. E., Cunha Neto, J. A. B., Philippi P. C. "Predicting Physical Properties of Reservoir Rocks from the Microstructural Analysis of Petrographic Thin Sections*"*. Produccion 2000 / Aplicaciones de la ciencia en la ingeniería de petróleo**,** May 08-12 /2000, Foz de Iguaçu

Frisch, U., Hasslacher B., Pomeau Y., 1986, Lattice-Gas Automata for the Navier-Stokes Equation, Physical Review Letters 56, 1505-1508.

Frisch, U., d'Humières, D., Hasslacher, B., Lallemand, P., Pomeau, Y. and Rivet, J., 1987, Lattice Gas Hydrodynamics in Two and Three Dimensions, Complex Systems 1, 649-707.

Hardy, J., Pomeau, Y., de Pazzis O., 1973, Time Evolution of a Two-Dimensional Model System. I. Invariant States and Time Correlation Functions, J. Math. Phys. 14, 1746-1759.

Higera, F. and Jimenez, J., 1989, Boltzmann approach to lattice gas simulations, Europhys. Lett. 9, 663-668.

d'Humières, D., Lallemand, P., and Frisch, U., 1986, Lattice gas models for 3D hydrodynamics, Europhys. Lett. 2, 291-297.

Liang, Z. R., Fernandes, C. P., Magnani, F.S. and Philippi, P. C., 1998, A Reconstruction Technique of 3-D Porous Media by using Image Analysis and Using Fourier Transform, Journal of Petroleum Science and Engineering, 21, 3-4, 273-283.

McNamara G. G. and Zanetti G., 1988, Use of the Boltzmann Equation to Simulate Lattice-Gas Automata, Physical Review Letters 61, 2332-2335.

Qian, Y., d'Humières, D., Lallemand, P., 1992, Lattice BGK models for Navier-Stokes equation, Europhys. Lett. 17, 345-349.

Rothman, D. H., Zaleski, S., 1997, Lattice-gas cellular automata: simple models of complex hydrodynamics , Cambridge University Press, Cambridge.

Zou, Q. and He, X., 1997, On pressure and velocity boundary conditions for the lattice Boltzmann BGK model, Phys. Fluids 9, 1591-1598.